Accounting for Environmental Effects in ab Initio Calculations of Proton Transfer Barriers

Markus A. Lill, Michael C. Hutter, and Volkhard Helms*

Max-Planck Institute of Biophysics, Kennedyallee 70, 60596 Frankfurt/Main, Germany

Received: April 24, 2000; In Final Form: June 21, 2000

The proton transfer between imidazole and water was studied by quantum chemical calculations in the presence of further ligand water molecules. In particular, we investigated the effect of the position of secondary waters relative to the proton transfer system. It is shown that the energy surface of transfer can be well reproduced when these waters are replaced by point charges. We found that at close distances the charges need to be enhanced to account for induced polarization. As a further simplification, the environmental effects of these secondary waters on the proton transfer barriers can be described analytically by the electrostatic interaction of fitted point charges placed at the position of the ligand waters using the Mulliken charges of imidazole and the primary water.

Introduction

Proton-transfer reactions are essential parts of numerous biochemical and bioenergetic processes, for example, in enzymatic reactions such as serine proteases,[1−3] or carbonic anhydrase[4] or in proton transport paths through entire membrane proteins such as bacteriorhodopsin[5] or cytochrome *c* oxidase.[6,7]

The thermodynamic and kinetic properties of proton transfer processes in proteins are strongly influenced by the environment of the proton-transferring chemical groups.[1−4] The relative energies of reactant and product states are modified predominantly through electrostatic interactions,[4] as is the energy barrier height between these two states. Environmental effects, therefore, have a significant impact on reaction rates and equilibria and on local pK_a values[8] of titratable residues.

Different theoretical approaches have been proposed to describe the environmental influence on proton transfer reactions. The most accurate and most costly approach is to treat the complete system of proton-transferring groups and their adjoining environment up to a defined distance by electronic structure methods.[9] QM/MM methods are being used to consider a larger part of the environment in an efficient manner and simultaneously to allow for a higher level of quantum mechanical description of the reactive groups. In these methods, the active center of the reaction is described fully quantum mechanically by electronic structure methods, whereas the environmental groups are treated using force field methods[10] or are described by a polarizable continuum in a self-consistent reaction field approach.[1]

However, even faster methods are necessary if one wants to study transport processes on much longer time scales and for large systems such as membrane proteins. An empirical force field approach was used previously by Brickmann and coworkers[11] to study liquid water with one excess proton, and proton transfer was described as instantaneous hopping. We would like to extend this approach to simulate protein systems by molecular dynamic simulations whereby proton transfer occurs between different titratable residues and water molecules. Thus, we need to derive an analytical description of hopping probabilities for every geometry of the proton-transferring and environmental groups, and this is the aim of this study. A proton-transfer model system is chosen consisting of a proton-donating amino acid side group, imidazole, and an accepting group, one water molecule, (Figure 1: system A) that has previously been studied by Lu and Voth.[4] In a subsequent paper, results will be presented for proton-transfer barriers between all titratable amino acids and water molecules.

The energy hypersurface, from which the transfer probabilities can be derived, is dependent on different parameters. First, the dependence of the proton-transfer energy surface on the distance between the donating and the accepting atom, here *R*(NO), is analyzed. Then the influence of environmental groups, here ligand water molecules, is investigated (Figure 1: systems B and C). The effect of the relative positions of these secondary waters to the proton-transferring imidazole−water system is analyzed. From these data, an analytical approach is derived in a stepwise manner, which accounts for the environmental effects on the proton-transfer energy surface.

Method of Calculation

The calculations were performed with the program package NWChem 3.1[12] on DEC alpha workstations. To establish the computational methodology, the proton transfer in the well studied system $H_5O_2^+$ was chosen as a test case. The results for different proton acceptor−donor distances with density functional methods (B3LYP functional) and wave function methods (MP2) using basis sets ranging from 3-21G to 6-31G** are shown in Table 1, together with those from very accurate coupled cluster calculations taken from ref 13. RHF results are in satisfactory agreement with those found in the literature.[14] As discussed in refs 13 and 15, density functional methods underestimate the energy barriers between the two minimum energy states compared to results obtained by CCSD(T) and QCISD(T) calculations. The predictions for the energy barriers derived with MP2 are closer to those of these high-level approaches. Therefore, we only show results from MP2 calculations for the imidazole−water system.

* To whom correspondence should be addressed.

10.1021/jp001550m CCC: $19.00
Published on Web 08/15/2000

TABLE 1: Energy Barriers [kcal/mol] for Proton Transfer in $H_5O_2^+$ at Different *R*(OO)

	R(OO) [Å]			
method	2.5	2.6	2.7	2.8
MP2/6-31G* // HF/3-21G	0.3	2.0	4.7	8.4
MP2/6-31G** // HF/6-31G**	0.4	2.1	5.7	10.0
B3LYP/6-31G* // HF/3-21G	0.1	1.2	3.5	6.6
B3LYP/6-31G** // HF/6-31G**	0.1	1.0	3.8	7.4
CCSD(T)/cc-pVTZ // MP2/cc-pVTZ[a]	0.37	2.08	4.85	8.44
QCISD(T)/cc-pVTZ // MP2/cc-pVTZ[a]	0.38	2.06	4.82	8.40

[a] Taken from ref 13.

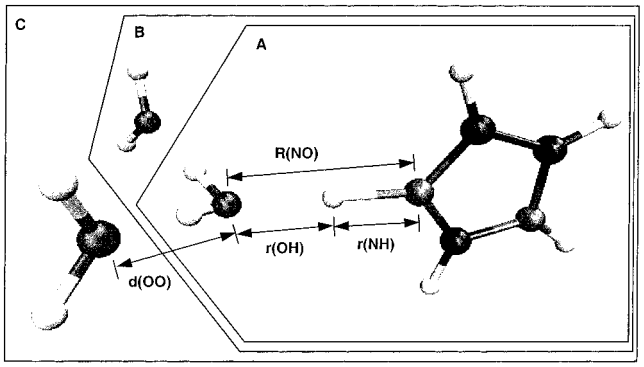

Figure 1. Proton-transfer system consisting of imidazole, a proton-accepting, primary water (system A), and one (system B) or two (system C) secondary, or ligand, waters. Four interatomic distances *r*(NH), *r*(OH), *R*(NO) and *d*(OO), which will be used as reaction criteria in this study, are labeled.

The geometries of system A (Figure 1), consisting of imidazole and water, are optimized using HF/6-31G**, and the energies are calculated at MP2/6-31G** // HF/6-31G**. To obtain the energy surface of a proton-transfer reaction, the proton is moved stepwise by 0.1 Å along the $N_{Im}-O_{Prim.Wat}$ interconnecting line. At each *r*(NH) the geometry is optimized, keeping the distance *R*(NO) and the angle ∠(NHO) fixed. All other degrees of freedom remain free.

When studying environmental effects, adding one (system B) or two secondary waters (system C), the geometries are optimized using HF/3-21G to save computing time, and the energies are calculated at MP2/6-31G*//HF/3-21G. In the optimization procedure, the coordinates for the oxygens of the secondary waters are first determined at an intermediate distance *r*(NH) = 1.4 Å while keeping the primary water fixed. Then, similar to system A, the energy is calculated at every *r*(NH) while constraining the coordinates of the donating atom N_{Im}, the transferred hydrogen, and the accepting $O_{Prim.Wat}$, as well as the position of the oxygen of the secondary waters.

Since systems B and C contain more basis functions than system A, the importance of the basis set superposition error was checked for a correct estimation of the effect of the secondary waters. This was done by Counterpoise Correction, that is, examining system A and ghost atoms with orbitals on the positions of the secondary waters. The energy surface compared to that of system A shows only negligible differences (results not shown).

Results and Discussion

Proton-Transfer Barriers without Secondary Water Molecules. The proton-transfer energy surface for the imidazole−water system is shown in Figure 2 as a function of the separation between the donating atom and transferred proton, *r*(NH), at different distances between donor and acceptor, *R*(NO), ranging from 2.65 Å to 3.15 Å. For large separations *R*(NO) ≥ 2.95 Å, a double-well potential is formed with a single deep minimum at about *r*(NH) = 1.03 Å, where the proton is bound to the donor N_{Im}, and a shallow minimum at about *r*(OH) = 1.09 Å (for *R*(NO) = 2.95 Å) to *r*(OH) = 1.05 Å (for *R*(NO) = 3.15 Å), where the proton can be assigned to the accepting $O_{Prim.Wat}$. The shape of the double-well potential reflects the stronger proton affinity of an imidazole group compared to that of a water molecule.[4] For *R*(NO) ≤ 2.95 Å, the proton affinity of the water molecule is insufficient to form a stable hydronium ion; the second minimum disappears.

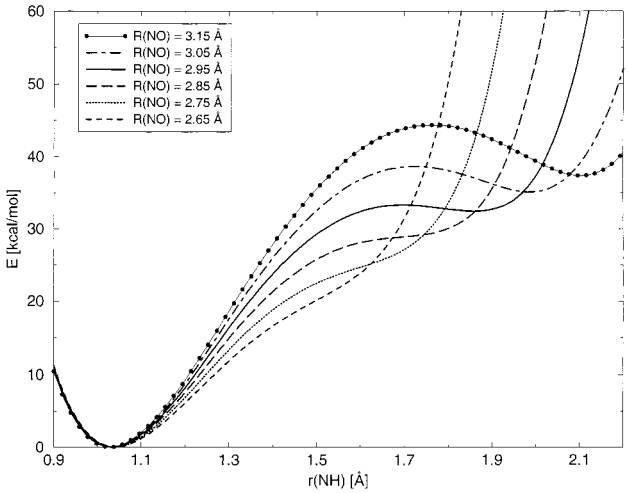

Figure 2. Proton-transfer energy surface for system A as a function of *r*(NH) at different separations between imidazole's nitrogen and the primary water's oxygen, *R*(NO) = 2.65 Å...3.15 Å.

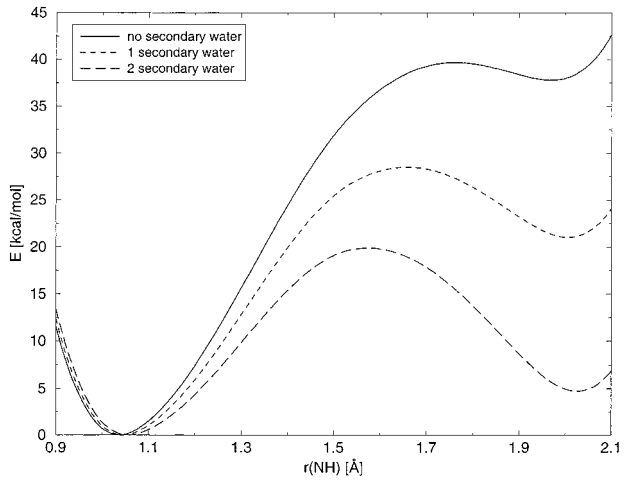

Figure 3. Influence of one and two secondary waters on the proton-transfer energy surface for imidazole−water at *R*(NO) = 3.05 Å and *d*(OO) = 2.6 Å.

Influence of Secondary Water Molecules on the Proton Transfer Barrier. As previously shown by Lu and Voth,[4] secondary water molecules ligated to the primary, proton-accepting water molecule stabilize the formation of H_3O^+ mainly by electrostatic interaction between the ligand waters and the changing charge distribution that accompanies the proton-transfer process. Figure 3, as one example, shows the effect of one and two secondary waters at a distance of *d*(OO) = 2.6 Å between primary and secondary water on the proton-transfer energy surface of the imidazole−water system at *R*(NO) = 3.05 Å. The stabilization of the second minimum results in a decrease of the forward energy barrier by 11 kcal/mol to about 29 kcal/mol for one ligand water and by 20 kcal/mol to about 20 kcal/

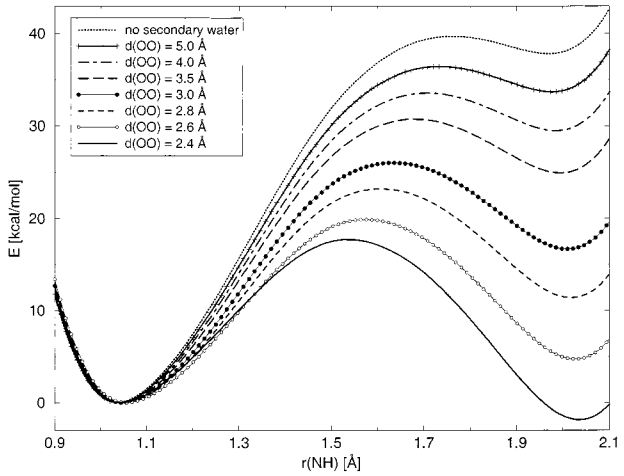

Figure 4. Dependence of energy barriers for system C on the position of the secondary waters relative to the primary water. The distance is varied from $d(\mathrm{OO}) = 2.4$ Å to $d(\mathrm{OO}) = 5.0$ Å and to infinity, which means no secondary waters are present. These calculations were performed at $R(\mathrm{NO}) = 3.05$ Å.

mol for two ligand waters. In addition, the proton-transfer barrier for the backward transfer from water to imidazole increases from about 2 kcal/mol to 8 kcal/mol for one and to 15 kcal/mol for two secondary waters.

The effect of varying the distance between primary and secondary waters is demonstrated in Figure 4. As the secondary waters are shifted away, the electrostatic interaction with the imidazole−water system and thus the stabilization of the second minimum diminishes. As a consequence, the barrier increases from 20 kcal/mol at $d(\mathrm{OO}) = 2.6$ Å to 36 kcal/mol at $d(\mathrm{OO}) = 5.0$ Å, while the barrier for the reverse transfer decreases from 15 kcal/mol at $d(\mathrm{OO}) = 2.6$ Å to 3 kcal/mol at $d(\mathrm{OO}) = 5.0$ Å.

Modeling of the Secondary Waters by Point Charges. The question now arises of whether the proton-transfer energy surface of the complete system C, consisting of proton donor (imidazole) and acceptor (water) under the influence of their environmental structure (secondary waters), can be reproduced by treating the isolated system A, proton donor and acceptor, with electronic structure methods (here, MP2) and by representing the secondary waters molecular mechanically as three point charges at the positions of the nucleic centers. To examine this situation, the explicit ligand waters were replaced by point charges, and single-point calculations were performed varying $r(\mathrm{NH})$, using the geometry of the complete system with explicit secondary waters optimized at the corresponding $r(\mathrm{NH})$ distance. The point charges of the hydrogen atoms of the waters are chosen to be identical, and the total charge on each water equals zero.

Figure 5 shows the energy profiles for $d(\mathrm{OO})$ ranging from 2.4 Å to 5.0 Å. For distances $d(\mathrm{OO}) \geq 5.0$ Å, the energy profiles computed with the simple point charge water model (SPC) of Berendsen and co-workers[19] ($q_\mathrm{O} = -0.82/q_\mathrm{H} = 0.41$, solid line) are in excellent agreement with those for the full quantum system (results for $d(\mathrm{OO}) = 6.0$ Å are not shown here). For shorter distances, one observes increasing deviations the closer the secondary waters approach the primary water. To reproduce the quantum mechanical energy barrier, the charges on the secondary waters had to be increased up to $q_\mathrm{O} = -1.20/q_\mathrm{H} = 0.60$. Table 2 shows that by systematically increasing the point charges, energy surfaces are obtained in excellent agreement with those obtained by calculations with quantum mechanically treated ligand waters.

As the secondary waters approach the primary water, the magnitude of the point charges that give the best fit increases

TABLE 2: Comparison Between Energy Barriers of the Fully Quantum Mechanically Treated System C with Systems in Which the Secondary Waters are Modeled by Point Charges

$d(\mathrm{OO})$ [Å]	point charges of best fit [e] $q_\mathrm{O}/q_\mathrm{H}$	$E_\mathrm{b}^{\rightarrow}$ [kcal/mol]		$E_\mathrm{b}^{\leftarrow}$ [kcal/mol]	
		QM waters	point charge waters	QM waters	point charge waters
2.6	−1.20/0.60	19.9	19.6	15.2	14.4
3.0	−1.10/0.55	26.0	25.8	9.3	8.7
3.5	−1.00/0.50	30.7	30.5	5.8	5.6
4.0	−0.90/0.45	33.5	33.5	4.0	4.0
5.0	−0.82/0.41	36.4	36.4	2.7	2.7
6.0	−0.82/0.41	37.7	37.7	2.4	2.4

continuously from $q_\mathrm{O} = -0.82/q_\mathrm{H} = 0.41$ at $d(\mathrm{OO}) = 5.0$ Å and $d(\mathrm{OO}) = 6.0$ Å to $q_\mathrm{O} = -1.20/q_\mathrm{H} = 0.60$ at $d(\mathrm{OO}) = 2.6$ Å. The closer a secondary water approaches the primary water, the stronger is the interaction between the dipole of the latter with the electron density of the ligand water. Therefore, the induced polarization of the secondary water and thus the absolute values of the charges on the nuclei positions increase.

For $d(\mathrm{OO}) = 2.4$ Å, the energy surface of the full quantum system cannot be reproduced by point charges on secondary waters anymore. This may be due to a strong polarization of the system, which leads to charged secondary water molecules. We found that Mulliken charges on the atoms of a secondary water sum up to a total charge varying from 0.03 e at $r(\mathrm{NH}) = 0.9$ Å to 0.08 e at $r(\mathrm{NH}) = 2.1$ Å, whereas the sum for $d(\mathrm{OO}) = 2.6$ Å varies only from 0.035 e at $r(\mathrm{NH}) = 0.9$ Å to 0.065 e at $r(\mathrm{NH}) = 2.1$ Å. This may explain why a neutral secondary water with equal charges for every $r(\mathrm{NH})$ is not able to reproduce the correct energy surface for the proton-transfer process.

For distances $d(\mathrm{OO}) \geq 2.6$ Å, it is feasible to calculate the proton-transfer surface between an amino acid side chain, here imidazole, and water surrounded by ligand waters, treating these molecular mechanically using point charges. Whereas for $d(\mathrm{OO}) \geq 5.0$ Å, charges of SPC water can be used, the charges of the ligand waters for $2.6\ \text{Å} \leq d(\mathrm{OO}) \leq 5.0$ Å should be enhanced by a factor that is dependent on $d(\mathrm{OO})$ (Figure 6).

Results for the fitted point charges at $R(\mathrm{NO}) = 2.65$ Å were very similar to those obtained at $R(\mathrm{NO}) = 3.05$ Å.

A water molecule represented by point charges of $q_\mathrm{O} = -1.20/q_\mathrm{H} = 0.60$ has a dipole moment of ca. 3.2 D. This may appear quite large when compared to the experimental value in a vacuum (ca. 1.8 D) or to the empirical SPC water (ca. 2.3 D). However, dipole moments as high as 2.9 D were previously reported in molecular dynamics simulations of bulk water with explicit polarizabilities.[16−18] Even higher values should be possible for a well-coordinated water molecule in a protein interior, for example.

Analytical Description of the Environmental Effects on the Proton-Transfer Barriers. In the previous section, it was shown that the environmental effect of secondary water molecules on a proton-transfer reaction can be well reproduced by treating the secondary waters as point charges with distance-dependent magnitudes, at least for $d(\mathrm{OO}) \geq 2.6$ Å. But it is still necessary to recalculate the energy surface of the proton transfer between isolated donor and acceptor for every rearrangement of the surrounding waters. A significant improvement would be if the proton-transfer energy surface only had to be calculated once for the isolated system (system A) and if the influence of surrounding ligand waters on the energy landscape could be added as a correction later on.

Table 3 and Figures 7a and 7b show the results of a stepwise approach to determining the energy surface of the complete

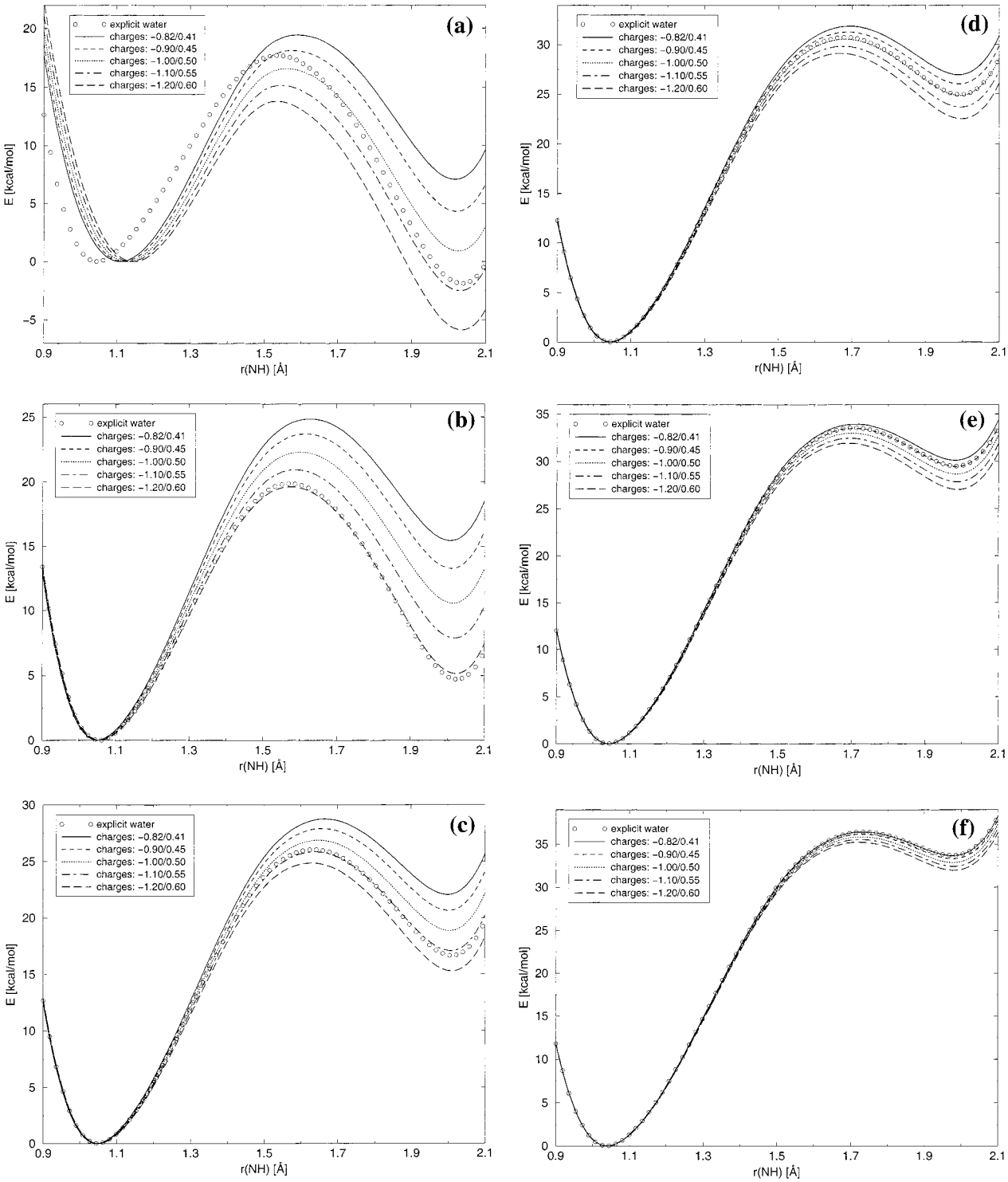

Figure 5. Comparison of the energy barriers for system C (where the secondary waters are part of the electronic structure calculation) with those having the ligand waters modeled by point charges. The point charges are varied between $q_O = -0.82/q_H = 0.41$(SPC) and $q_O = -1.20/q_H = 0.60$. The distance between imidazole and primary water is R(NO) = 3.05 Å. Comparisons are shown for distances between primary and secondary waters ranging from (a) d(OO) = 2.4 Å, (b) d(OO) = 2.6 Å, (c) d(OO) = 3.0 Å, (d) d(OO) = 3.5 Å, (e) d(OO) = 4.0 Å to (f) d(OO) = 5.0 Å.

system C, by adding the electrostatic interaction energy between ligand waters and the imidazole−water system A to the energy landscape of system A for the cases d(OO) = 2.6 Å and d(OO) = 3.0 Å at R(NO) = 3.05 Å. This approach was motivated by the work of Borgis,[20] who derived a dipole approximation to estimate the effect of an external electric field **E** on the proton transfer barrier between two water molecules.

In a first step, using the geometry and the Mulliken charges of the optimized system C, electrostatic interaction between the Mulliken charges of donor and acceptor Q_i (i = 1, ..., 13) and electrostatic potential Φ created by the point charges of the secondary waters q_j (j = 14, ..., 19) is calculated according to

$$E_{el} = \sum_{i=1}^{13} Q_i \Phi(\mathbf{r_i}) \tag{1}$$

$$= \sum_{i=1}^{13} Q_i \sum_{j=14}^{19} \frac{q_j}{4\pi\epsilon_0 |\mathbf{r_i} - \mathbf{r_j}|} \tag{2}$$

TABLE 3: Energy Barriers for Different Approaches, in Increasing Order of Simplification

point charges on 2nd H_2O [e]			$d(OO) = 2.6$ Å $q_O = -1.20/q_H = 0.60$		$d(OO) = 2.8$ Å $q_O = -1.20/q_H = 0.60$	
1st H_2O, imidazole[a]	2nd H_2O[b]	energy calculation[c]	$E_b^{\rightarrow}$ [kcal/mol]	$E_b^{\leftarrow}$ [kcal/mol]	$E_b^{\rightarrow}$ [kcal/mol]	$E_b^{\leftarrow}$ [kcal/mol]
QM	QM	MP2	19.9	15.2	23.2	11.8
QM	MM	MP2	19.6	14.4	22.6	11.5
MM_C	MM	all multipoles	20.1	15.0	23.3	11.4
MM_C	MM	dipole	23.2	10.5	26.0	9.1
MM_A	MM	all multipoles	21.7	10.8	24.4	9.3
MM_A	MM	dipole	25.1	11.3	27.3	9.5
point charges on 2nd H_2O [e]			$d(OO) = 3.0$ Å $q_O = -1.10/q_H = 0.55$		$d(OO) = 3.5$ Å $q_O = -1.00/q_H = 0.50$	
1st H_2O, imidazole	2nd H_2O	energy calculation	$E_b^{\rightarrow}$ [kcal/mol]	$E_b^{\leftarrow}$ [kcal/mol]	$E_b^{\rightarrow}$ [kcal/mol]	$E_b^{\leftarrow}$ [kcal/mol]
QM	QM	MP2	26.0	9.3	30.7	5.8
QM	MM	MP2	25.8	8.7	30.5	5.6
MM_C	MM	all multipoles	27.1	8.6	31.9	5.6
MM_C	MM	dipole	28.9	7.2	32.4	5.2
MM_A	MM	all multipoles	27.4	7.3	31.9	5.1
MM_A	MM	dipole	29.8	7.7	32.8	5.3

[a] QM: imidazole and primary water are treated quantum mechanically; $MM_{C/A}$: Geometry and Mulliken charges are taken from electronic structure calculation on system C/A. [b] Ligand waters are treated quantum mechanically (QM) or are modeled by point charges (MM). [c] The energy surface is determined by electronic structure calculations (MP2), by eq 2 where all multipoles are taken into account, or by eq 4 where just the dipole term is considered.

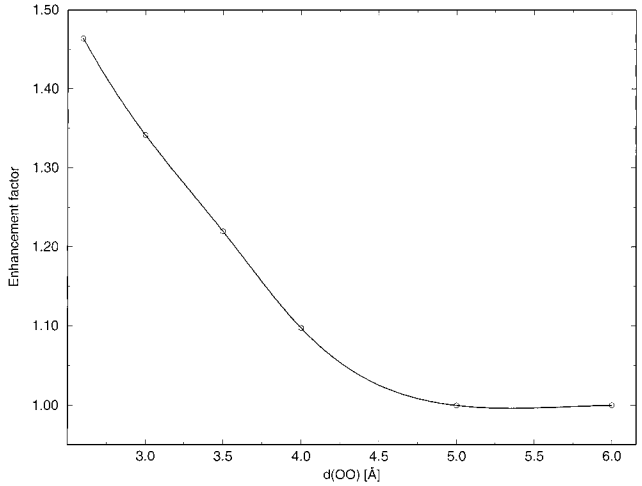

Figure 6. Factor by which the SPC charges of the ligand waters have to be enhanced to give the best fit for the proton-transfer energy barrier at a specific d(OO).

This electrostatic energy is added to the energy surface of the proton transfer in the isolated system A. Using charges of $q_O = q_{14} = q_{17} = -1.2$ and $q_H = q_{15} = q_{16} = q_{18} = q_{19} = 0.6$ for d(OO) = 2.6 Å, the resulting energy curve (Figure 7a: solid line with open diamonds) is in very good agreement with the curve of system C (solid line). For d(OO) = 3.0 Å, using $q_O = -1.1$ and $q_H = 0.55$, the maximal error is about 1 kcal/mol (Figure 7b). The same remarkable agreement is also found for d(OO) = 2.8 Å and d(OO) = 3.5 Å (Table 3). Therefore, the interaction between the quantum mechanically treated part A and the point charges on the secondary waters can be reduced to the energy expression (eq 2), in which the electronic structure part A is also treated by point charges, here, as Mulliken charges on the nucleic centers. The geometry and the Mulliken charges of the complete system C, however, are still being used.

The next step is to employ the optimized geometry and the Mulliken charges of system A instead of system C. Only the positions of the secondary waters are taken from the optimized structure of system C. The electrostatic energy is calculated as described above and is added to the energy curve of system A. The result (solid line with filled circles) for d(OO) = 2.6 Å deviates from the fully quantum mechanically calculated curve (solid line) by 1.8 kcal/mol for $E_b^{\rightarrow}$ and by 4.4 kcal/mol for $E_b^{\leftarrow}$. Compared to the overall effect of the two secondary waters, which led to a reduction of the barrier of the isolated system by 20 kcal/mol for $E_b^{\rightarrow}$ and an increase by 13 kcal/mol for $E_b^{\leftarrow}$, a deviation by 1.8 kcal/mol for $E_b^{\rightarrow}$ is still satisfactory, whereas the discrepancy of 4.4 kcal/mol for $E_b^{\leftarrow}$ is quite high. This tendency (the deviation for $E_b^{\leftarrow}$ is larger than for $E_b^{\rightarrow}$) is also found at d(OO) = 2.8 Å and d(OO) = 3.0 Å and results from the strong interaction between the hydronium ion and the close secondary waters that stabilize the ion by influencing its geometry and charge distribution. As $d(OO)$ is increased, the error compared to the absolute effect of the environment reduces to about 10%, as shown in Table 3 for d(OO) = 3.5 Å.

In a final step of simplification, the calculation of the electrostatic energy was replaced by their first-order Taylor expansion, the dipole approximation, as discussed by Borgis et al.[20] for the proton transfer between two water molecules under the influence of an external electric field **E**. Expanding the potential Φ around a point $\mathbf{r_0}$

$$\Phi(\mathbf{r}) = \Phi(\mathbf{r_0}) - (\mathbf{r} - \mathbf{r_0})\mathbf{E}(\mathbf{r_0}) - \frac{1}{2}\sum_{k=x,y,z}\sum_{l=x,y,z}(r^k - r_0^k)(r^l - r_0^l)\frac{\partial E^l}{\partial r^k}(\mathbf{r_0}) + \ldots \quad (3)$$

leads in first order to an electrostatic interaction energy:

$$E_{el}^{(1)} = \sum_{i=1}^{13} Q_i \sum_{j=14}^{19} \frac{q_j}{4\pi\epsilon_0|\mathbf{r_0} - \mathbf{r_j}|} - \sum_{i=1}^{13} Q_i(\mathbf{r}_i - \mathbf{r_0}) \sum_{j=14}^{19} \frac{q_j(\mathbf{r_0} - \mathbf{r_j})}{4\pi\epsilon_0|\mathbf{r_0} - \mathbf{r_j}|^3} \quad (4)$$

This expression was evaluated for the optimized geometry and Mulliken charges of system C. The midpoint between the

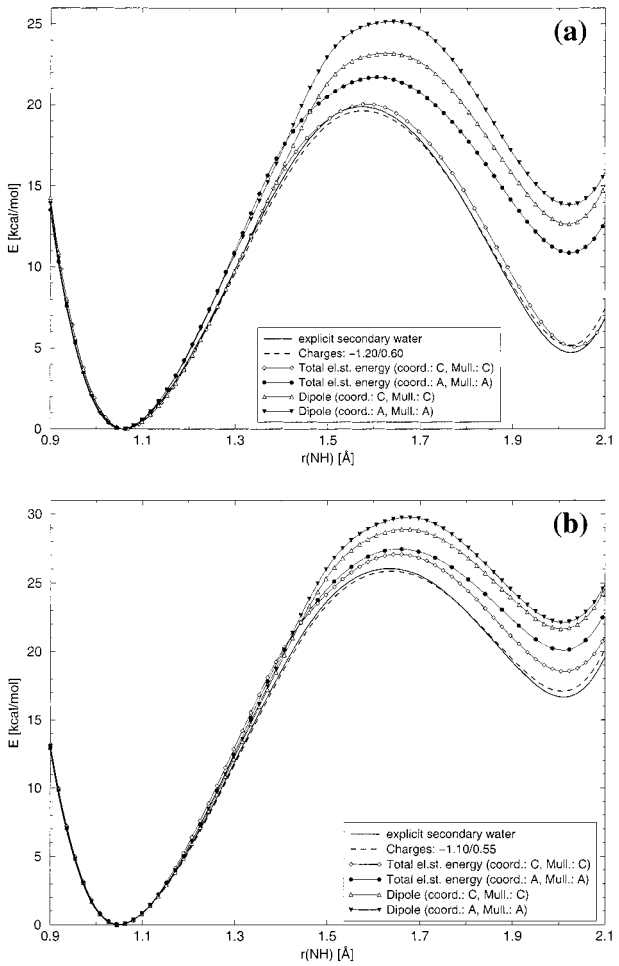

Figure 7. Energy surfaces where the effect of the secondary waters is calculated with formula (2). Mulliken charges and geometries of imidazole and primary water are taken from electronic structure calculations on system C (solid line with open diamonds) or on system A, (solid line with filled circles), or with formula (4) (solid line with open triangles or filled trangles, respectively, for Mulliken charges and geometries as described previously). Again, $R(\mathrm{NO}) = 3.05$ Å. Results are shown (a) for $d(\mathrm{OO}) = 2.6$ Å and (b) for $d(\mathrm{OO}) = 3.0$ Å.

donating nitrogen atom of imidazole and the accepting oxygen atom of the primary water was chosen as $\mathbf{r_0}$. As can be seen in Figure 7 (solid line with open triangles) the deviations for this dipole approximation from the energy surface of system C, calculated by the electronic structure method (solid line), are significantly larger than for the complete electrostatic interaction. The differences are $\Delta E_{\mathrm{b}}^{\rightarrow} = 3.3$ kcal/mol and $\Delta E_{\mathrm{b}}^{\leftarrow} = 4.7$ kcal/mol. Whereas the dipole approximation gives excellent results for system A under the influence of a homogeneous electric field (results not shown), the effect of the inhomogeneous electric potential produced by secondary waters, close in distance to the donor−acceptor system, cannot be well described just using the dipole approximation. For $d(\mathrm{OO}) \geq 3.5$ Å, the effect of the multipoles higher than the dipole decreases, and energy barriers calculated with the electric field−dipole term approximate those of the complete electrostatic interaction. Thus, the dipole approximation seems to be an efficient way to describe the effect of environmental groups at distances of more than 3.5 Å from the accepting group, and higher multipoles should be used to describe the effect of secondary waters in hydrogen-bonding distances.

Conclusions

The results presented show that the nature and the geometry of the surrounding hydrogen-bonded ligand waters significantly influence the energy surface of the proton transfer reaction studied. Thus, one has to be aware of this when neglecting the environment of proton transferring groups and more generally of sites where chemical reactions occur. Since it is computationally very expensive to use electronic structure methods to describe the chemically reactive groups together with a large environment, a QM/MM approach provides, in principle, an effective alternative to treat such problems.

We have demonstrated that it is possible to determine the energy surface of a proton transfer reaction between an amino acid, here a histidine side chain, and a water molecule that is coordinated by secondary ligand waters by calculations of only the proton donating and accepting groups with electronic structure methods, while treating the environment, here the secondary waters, as point charges. The only correction necessary, due to polarization effects between the hydrogen-bonded water molecules, is to enhance the charges of the point particle waters by a factor that depends on the distance between primary and secondary waters.

For environmental groups not strongly hydrogen bonded to the accepting water molecule, one can go one step further. After calculating a wave function for the isolated system consisting of proton donor and acceptor, the effect of the environmental charges is added subsequently by calculating the electrostatic interaction energy between proton transferring groups and the surrounding point charges. It is thus possible to study the influence of different environments on a specific reaction in a very simple and fast manner.

It remains to be seen in the future how well this QM/MM approach works for ligands other than water and for other chemical reactions. A future publication will test the approach to describe the phosphoryl transfer reaction in protein kinases. Then it would suffice to compute by electronic structure methods the energy landscape only including the groups that are directly involved in the chemical reaction studied. Afterward, the influence of a surrounding protein matrix or solvent can be added by considering just the electrostatic interaction between reactive part and environment.

Acknowledgment. NWChem Version 3.3, as developed and distributed by Pacific Northwest National Laboratory, P.O. Box 999, Richland, WA 99352 and funded by the U.S. Department of Energy, was used to obtain some of these results.

References and Notes

(1) Li, G.-S.; Maigret, D.; Rinaldi, D.; Ruiz-López, F. *J. Comput. Chem.* **1998**, *19*, 1675.

(2) Warshel, A.; Naray-Szabo, G.; Sussman, F.; Hwang, J.-K. *Biochemistry* **1989**, *28*, 3629.

(3) Umeyama, H.; Hirono, S.; Nakagawa, S. *Proc. Natl. Acad. Sci. U.S.A.* **1984**, *81*, 6266.

(4) Lu, D.; Voth, G. A. *J. Am. Chem. Soc.* **1998**, *120*, 4006.

(5) Luecke, H.; Schobert, B.; Richter, H. T.; Cartailler, J.-P.; Lanyi, J. K. *Science* **1999**, *286*, 255.

(6) Iwata, S.; Ostermeier, C.; Ludwig, B.; Michel, H. *Nature (London)* **1995**, *376*, 660.

(7) Michel, H. *Biochemistry* **1999**, *46*, 15129.

(8) Kannt, A.; Lancaster, C. R. D.; Michel, H. *Biophys. J.* **1998** *74*, 708.

(9) Hutter, M. C.; Helms, V. *Protein Sci.* **1999**, *8*, 2728.

(10) Cunningham, M. A.; Ho, L. L.; Hguyen, D. T.; Gillilan, R. E.; Bash, P. A. *Biochemistry* **1997**, *36*, 4800.

(11) Schmidt, R. G.; Brickmann, J. *Ber. Bunsen-Ges. Phys. Chem.* **1997**, *101*, 1816.

(12) High Performance Computational Chemistry Group. *NWChem, A Computational Chemistry Package for Parallel Computers*, Version 3.3; Pacific Northwest National Laboratory: Richland, WA, 1998.
(13) Sadhukhan, S.; Muñoz, D.; Adamo, C.; Scuseria, G. E. *Chem. Phys. Lett.* **1999**, *306*, 83.
(14) Duan, X.; Scheiner, S.; Wang, R. *Int. J. Quantum Chem., Quantum Biol. Symp.* **1993**, *20*, 77.
(15) Barone, V.; Orlandini, L.; Adamo, C. *Chem. Phys. Lett.* **1994**, *231*, 295.
(16) Ahlström, P.; Wallqvist, A.; Engström, S.; Jönson, B. *Mol. Phys.* **1989**, *68*, 563.
(17) Sprik, M.; Klein, M. L.; Watanabe, K. *J. Phys. Chem.* **1990**, *94*, 6483.
(18) Nymand, T. M.; Linse, P. *J. Chem. Phys.* **2000**, *112*, 6386.
(19) Berendsen, H. J. C.; Postma, J. P. M.; van Gunsteren, W. F.; Hermans, H. J. In *Intermolecular Forces*; Pullman, B., Ed.; Reidel: Dordrecht, 1981; p 331.
(20) Borgis, D.; Tarjus, G.; Azzouz, H. *J. Chem. Phys.* **1992**, *97*, 1390.